



1 Inter-comparison study of atmospheric ^{222}Rn and ^{222}Rn 2 progeny monitors

3 Claudia Grossi^{1,2}, Olivier Llado³, Felix R. Vogel⁴, Victor Kazan³, Alessandro Capuana⁵,
4 Scott D. Chambers⁶, Sylvester Werczynski⁶, Roger Curcoll^{7,8}, Marc Delmotte³, Arturo
5 Vargas¹, Josep-Anton Morgui^{7,9}, Ingeborg Levin⁵, Michel Ramonet³.

6 ¹ Institut de Tècniques Energètiques (INTE), Universitat Politècnica de Catalunya (UPC), Barcelona,
7 Spain;

8 ² Physics Department, Universitat Politècnica de Catalunya (UPC), Barcelona, Spain;

9 ³ Laboratoire des Sciences du Climat et de l'Environnement, Université Paris-Saclay (LSCE/IPSL, CEA-
10 CNRS-UVSQ), Gif-sur-Yvette, France;

11 ⁴ Climate Research Division, Environment and Climate Change Canada, Toronto, Canada;

12 ⁵ Institut für Umweltphysik (IUP), Heidelberg University, Heidelberg, Germany;

13 ⁶ Environmental Research, ANSTO, Lucas Heights, Australia;

14 ⁷ Institut de Ciència i Tecnologia Ambientals (ICTA), Universitat Autònoma de Barcelona (UAB),
15 Cerdanyola del Vallès, Spain;

16 ⁸ Chemical Department, Universitat Politècnica de Catalunya (UPC), Barcelona, Spain;

17 ⁹ Departament Biologia Evolutiva, Ecologia i Ciències Ambientals, Universitat de Barcelona (UB),
18 Barcelona, Spain.

19 *Correspondence to:* Claudia Grossi (Claudia.grossi@upc.edu)

20 **Abstract.**

21 The use of the noble gas radon (^{222}Rn) as tracer for different research studies, for example observation-
22 based estimation of greenhouse gas (GHG) fluxes, has led to the need of high-quality ^{222}Rn activity
23 concentration observations with high spatial and temporal resolution. So far a robust metrology chain for
24 these measurements is not yet available.

25 A 3-month inter-comparison campaign of atmospheric ^{222}Rn and ^{222}Rn progeny monitors based on
26 different measurement techniques was realized during the fall and winter of 2016-2017 to evaluate: i)
27 calibration and correction factors between monitors necessary to harmonize the atmospheric radon
28 observations; and ii) the dependence of each monitor's response in relation to the sampling height,
29 meteorological and atmospheric aerosol conditions.

30 Results of this study have shown that: i) all monitors were able to reproduce the atmospheric radon
31 variability on daily basis; ii) linear regression fits between the monitors exhibited slopes between 0.62



32 and 1.17 and offsets ranging between -0.85 Bq m^{-3} and -0.23 Bq m^{-3} when sampling 2 m above ground
33 level (a.g.l.). Corresponding results at 100 m a.g.l. exhibited slopes of 0.94 and 1.03 with offsets of -0.13
34 Bq m^{-3} and 0.01 Bq m^{-3} , respectively; iii) no influence of atmospheric temperature and relative humidity
35 on monitor responses was observed for unsaturated conditions; and iv) changes of the ratio between radon
36 progeny and radon monitor responses were observed under very high atmospheric humidity and under
37 very low atmospheric aerosol concentrations. However, a more statistically robust evaluation of these last
38 influences based on a longer dataset should be conducted to improve the harmonization of the data.

39 Key words: radon, activity concentration, atmosphere, one-filter, two-filters, electrodeposition

40 1 Introduction

41 Over continents, the natural radioactive noble gas radon (^{222}Rn) (half-life $T_{1/2} = 3.8$ days) is continuously
42 generated within the soil because of the decay of radium (^{226}Ra) (Nazaroff and Nero, 1988; Porstendörfer,
43 1994) and it can then escape into the atmosphere by diffusion, depending on soil characteristics and
44 meteorological conditions (Grossi et al., 2011, Lopez-Coto et al., 2013; Karstens et al., 2015). The global
45 ^{222}Rn source into the atmosphere is mainly restricted to land surfaces (Szegevary et al., 2009; Karstens et
46 al., 2015), with the ^{222}Rn flux from water surfaces considered negligible for most applications (Schery
47 and Huang, 2004).

48 In recent decades the atmospheric scientific community has been addressing different research topics
49 using ^{222}Rn as a tracer. Examples of such applications include: the improvement of inverse transport
50 models (Hirao et al., 2010), the improvement of chemical transport models (Jacob and Prather, 1990;
51 Chambers et al. 2019a), the study of atmospheric transport and mixing processes within the planetary
52 boundary layer (Zahorowski et al., 2004; Galmarini, 2006; Baskaran, 2011; Chambers et al., 2011, 2019b;
53 Williams et al., 2011, 2013; Vogel et al. 2013; Vargas et al., 2015; Baskaran, 2016), the experimental
54 estimation of greenhouse gas (GHG) fluxes (Levin et al., 1999; 2011; Vogel et al., 2012; Wada et al.,
55 2013; Grossi et al., 2018), and others listed in Grossi et al. (2016).

56 In light of this, atmospheric ^{222}Rn measurements have been carried out at numerous monitoring stations
57 of GHG concentrations and air quality using three fundamentally different measurement principles: one
58 filter; two filters; and electrostatic deposition (Stockburger and Sittkus, 1966; Polian, 1986; Hopke, 1989;
59 Whittlestone and Zahorowski, 1998; Paatero et al., 1998; Levin et al., 2002). The two most commonly
60 employed measurement systems at European ^{222}Rn monitoring stations are: the dual-flow-loop two-filter
61 monitor (Whittlestone and Zahorowski, 1998; Zahorowski et al. 2004; Chambers et al., 2011, 2014,
62 2018; Griffith et al., 2016), which samples and measures radon directly, and the one-filter monitors, of
63 which several kinds are in use (e.g. Stockburger and Sittkus, 1966; Polian, 1986; Paatero et al., 1998;
64 Levin et al., 2002), which sample and measure aerosol-bound radon progeny. Finally, a third method is
65 being used at several Spanish atmospheric stations (Vargas et al., 2015; Hernández-Ceballos et al., 2015;
66 Grossi et al., 2016; Frank et al., 2016; Grossi et al., 2018; Gutiérrez-Álvarez et al., 2019). This type of
67 instrument performs a direct measurement of ^{222}Rn and ^{220}Rn (thoron) activity concentrations using
68 electrostatic deposition of ^{218}Po and ^{216}Po , respectively (Hopke, 1989; Grossi et al., 2012).



69 The diversity of the three aforementioned measurement techniques could introduce biases or
70 compatibility issues that would limit the comparability of the results obtained by independent studies and
71 the subsequent application of atmospheric radon data for regional-to-global investigations (e.g.
72 Schmithüsen et al., 2017). Thus, a comparative assessment of all the experimental techniques applied for
73 atmospheric ^{222}Rn activity concentration measurements and a harmonization of their datasets is needed, as
74 suggested by the International Atomic Energy Agency (IAEA, 2012).

75 Xia et al., 2010 carried out a comparison of the response of a dual-flow-loop two-filter detector from the
76 Australian Nuclear Science and Technology Organisation (ANSTO, Whittlestone and Zahorowski 1998)
77 and a one-filter monitor (α/β Monitor P3) manufactured by the Bundesamt für Strahlenschutz, Germany
78 (BfS) (Stockburger and Sittkus, 1966), for atmospheric ^{222}Rn measurements under various meteorological
79 conditions at 2.5 m above ground level (a.g.l.) over one year. Their results showed that both systems
80 followed the same patterns and produced very similar results most of the time, except under specific
81 meteorological conditions such as when precipitation or the proximity of the forest canopy could remove
82 short-lived progeny from the air mass to be measured by the one-filter monitor. However, Xia et al.
83 (2010) did not find a clear relationship between precipitation intensity and the ratio between progeny-
84 derived ^{222}Rn and ^{222}Rn activity concentration to convert the progeny signal to ^{222}Rn activity
85 concentration.

86 Grossi et al. (2016) presented results from two short (about 7-9 days) comparisons between a one-filter
87 monitor from Heidelberg University (HRM; Levin et al., 2002), and an Atmospheric Radon MONitor
88 (ARMON, Grossi et al., 2012), an electrostatic deposition monitor from the Universitat Politècnica de
89 Catalunya (UPC). The two comparison campaigns were carried out at a coastal and a mountain site, with
90 sampling in both cases from 10 m a.g.l. These comparisons revealed that the responses of both monitors
91 were in agreement except for water saturated atmospheric conditions or periods of rainfall. Again, the
92 quantity of comparison data was not sufficient to confirm any statistical correlation.

93 Loss of aerosols in the air intake systems can also complicate the derivation of ^{222}Rn activity
94 concentrations from one-filter systems such as the HRM. Levin et al. (2017) carried out an assessment of
95 ^{222}Rn progeny loss in long tubing by laboratory and field experiments. Results of these experiments, for
96 8.2 mm inner diameter (ID) Decabon tubing, gave an empirical correction function for ^{222}Rn progeny
97 measurements, which enables the correction of measurements for this specific experimental setup (tubing
98 type and diameter, flow rate, aerosol size distribution).

99 Finally, Schmithüsen et al. (2017) conducted an extensive European-wide $^{222}\text{Rn}/^{222}\text{Rn}$ progeny
100 comparison study in order to evaluate the comparative performance of one-filter and two-filter
101 measurement systems, determining potential systematic biases between them, and estimating correction
102 factors that could be applied to harmonize ^{222}Rn activity concentration estimates for their use as a tracer
103 in various atmospheric applications. In this case, the authors employed a reference HRM monitor, which
104 was taken to nine European measurement stations to run for at least one month at each of them. This
105 reference monitor was run in parallel to other one-filter and the two-filter radon monitors operating at
106 each station of interest.



107 Although several intercomparison campaigns have been carried out so far, none of them has included
108 simultaneous observations from one-filter, two-filter and electrostatic deposition methods. Here, we
109 present the results of a three-months intercomparison campaign carried out in the fall and winter of 2016-
110 2017 in Gif Sur Yvette (France) where, for the first time, co-located measurements from monitors based
111 on the three measurement principles were included. Two two-filter ^{222}Rn monitors, two single-filter ^{222}Rn
112 progeny monitors and an electrodeposition monitor were run simultaneously under different
113 meteorological and aerosol conditions sampling from heights of 2 and 100 m a.g.l.

114 The main objectives of the present study were to: i) compare the calibration and correction factors
115 between all monitors required to derive harmonized atmospheric radon activity concentrations; and ii)
116 analyze the influence that meteorological and environmental parameters, as well as sampling height, can
117 have on the finally determined ^{222}Rn activity concentration.

118 In the present manuscript the applied methodology is reported, including a short presentation of the
119 radon/radon progeny monitors participating in the campaigns, the sampling sites and the statistical
120 analysis carried out. Finally, the results of the study are presented and discussed.

121 **2 Methods**

122 In section 2.1 a short description is given of the monitors compared in the experiment, mainly focusing on
123 measurement techniques, instrument calibration and maintenance. The main characteristics of these
124 monitors are then summarized in Table 1. Section 2.2 presents the French atmospheric stations of Orme
125 de Mérisiers (ODM) and Saclay (SAC) where the two phases of the intercomparison campaign were
126 realized. Section 2.3 shortly described the devices used to measure the environmental parameters and the
127 atmospheric aerosol concentration at this previous sites during the experiment. Finally, the statistical
128 analysis applied is described in section 2.3.

129 **2.1 ^{222}Rn and ^{222}Rn progeny monitors**

130 **2.1.1 Dual-flow-loop two-filter detectors**

131 The two 1500 L dual-flow-loop two-filter detectors included in this exercise were designed and built at
132 the Australian Nuclear Science and Technology Organisation (ANSTO). This model of detector, which
133 will henceforth be named ANSTO, is based on a previous design by Thomas and Leclare (1970), with
134 some early iterations of the modified design being described by Whittlestone and Zahorowski (1998) and
135 Brunke et al. (2002). The subsequent evolution of two-filter detectors in recent decades, and the current
136 principle of operation, has been described in detail by Williams and Chambers (2016) and Griffiths et al.
137 (2016).

138 During the measurement campaign ambient air was sampled continuously at a rate of 83 L min^{-1} through
139 a 50 mm ID HDPE inlet tube and a 400 L delay volume to allow decay of the short-lived ^{220}Rn ($T_{1/2}= 56$
140 s). The air stream then passes through the first filter, which removes all ambient aerosols as well as ^{222}Rn
141 and ^{220}Rn progeny. The filtered sample, now containing only aerosol-free air and ^{222}Rn gas, enters the
142 main delay volume (1500 L) where ^{222}Rn decay produces new progeny. The newly formed ^{218}Po and
143 ^{214}Po are then collected on a second filter and their subsequent α decays are counted with a ZnS



144 photomultiplier system. Atmospheric ^{222}Rn activity concentrations are then calculated from the α count
145 rate and the flow rate through the chamber.

146 The detection limit of two-filter detectors is directly related to the volume of the main delay chamber. The
147 lower limit of detection of the 1500 L model used in this study was around 0.03 Bq m^{-3} . Under normal
148 operation ANSTO monitors are automatically calibrated in situ every month by injecting radon into the
149 sampling air stream from a well-characterized Pylon ^{226}Ra source (ca. 41 kBq radium at SAC station) for
150 5 hours at a fixed flow rate of $\sim 100 \text{ cc min}^{-1}$. Automatic instrumental background checks, each lasting 24
151 hours, are also performed every 3 months to keep track of long-lived ^{210}Pb accumulation on the detectors
152 second filter (which should be changed every 5 years). Based on a calibration source uncertainty of 4%,
153 coefficient of variability of valid monthly calibrations of 2-6%, and a counting uncertainty of around 2%
154 for radon concentrations $\geq 1 \text{ Bq m}^{-3}$, the total measurement of 1500 L ANSTO radon detectors is typically
155 8-12%.

156 Two ANSTO monitors were used during this study. As explained later in the text these monitors are
157 permanently running at SAC and ODM stations. No calibration source was available when the ANSTO
158 monitor was installed at the ODM site, so calibration and background information derived prior to
159 transport have been used. The ANSTO monitors have low-maintenance requirements but, due to their
160 dimensions (2.5 – 3m long) it can be challenging to install them at stations with space restrictions. As an
161 alternative to the 1500 L detectors, a 700 L model is also available, which is more portable and has a
162 detection limit of around 0.04 Bq m^{-3} .

163 2.1.2 One-filter monitors

164 One-filter detectors measure the decay rates of aerosol-bound ^{222}Rn progeny directly accumulated by air
165 filtration (Schmithüsen et al., 2017). The ^{222}Rn activity concentration is then calculated assuming a
166 constant disequilibrium factor (F_{eq}) for a given site and sampling height between ^{222}Rn and the measured
167 progeny in the sampled air.

168 In the present study two monitors based on this method were used. One was developed at the Institute of
169 Environmental Physics of Heidelberg University, Germany, and is described in detail by Levin et al.
170 (2002). Rosenfeld (2010) describe the most recent version of this monitor for which the electronics, data
171 acquisition, and evaluation hardware and software have been modernized. The HRM measurement is
172 based on α spectrometry of ^{222}Rn daughters attached to atmospheric aerosols collected on a static quartz
173 fiber filter (QMA \varnothing 47 mm) using a surface barrier detector (Canberra CAM 900 mm^2 active surface).
174 The detection limit of the HRM is about 0.05 Bq m^{-3} at a flow rate of about 20 L min^{-1} with an
175 uncertainty below $\pm 20\%$ for typical continental atmospheric ^{222}Rn levels above 1 Bq m^{-3} . In the
176 Saclay experiment, where air for the HRM was collected via a 100 m Decabon tubing (see below), the
177 line loss correction of Levin et al. (2017) was applied to all data. No loss of aerosol was assumed in the
178 short tubing used at Orme de Mérisiers station. Since one-filter detectors have no need for any delay
179 chambers but use only a compact filter holder with integrated detector and pre-amplifier, the HRM is a
180 small instrument and therefore easily portable. Regarding maintenance requirements, the quartz fiber
181 filter should be changed monthly.



182 The second type of one-filter monitor participating in this study was built at the Laboratoire des Sciences
183 du Climat et de l'Environnement, LSCE, France (Polian, 1986; Biraud, 2000; Schmithüsen et al., 2017).
184 Within this manuscript this monitor will be called the LSCE monitor. This monitor uses a moving filter
185 band system, which allows the determination of atmospheric ^{222}Rn activity concentration based on
186 measurements of its progeny ^{218}Po and ^{214}Po . Attached ^{222}Rn progeny are collected on a cellulose filter
187 (Pöllman–Schneider) over a one-hour period at a flow rate of 160 L min^{-1} and after this aerosol sampling
188 period, the loaded filter is moved to the alpha spectrometry for a one hour measurement period by a
189 scintillator from Harshaw Company and photomultiplier from EMI, Electronics Ltd (Biraud, 2000). The
190 minimum detection activity is about 0.01 Bq m^{-3} with an uncertainty of 20%.

191 Regarding maintenance on regular basis, the LSCE monitor's filter roll has to be changed every three
192 weeks. Automatic detector background is performed every three weeks and counting efficiency is
193 manually tested with an americium source. The instrument is designed to measure radioactive aerosols a
194 few meters above the ground level. An inlet filter is installed to avoid radon daughters on the main filter
195 roll. In addition, the filter also blocks black carbon or dirt deposition when the instrument is installed in
196 urban areas as the flow rate drops below $9\text{ m}^3\text{ h}^{-1}$. The instrument size is about 25 cm high, 40 cm long
197 and 25 cm deep, and it can be easily deployed at a station.

198 2.1.3 Electrostatic deposition monitor

199 The Atmospheric Radon Monitor (ARMON) used in this experiment was designed and built at the Institut
200 de Techniques Energétiques (INTE) of the UPC. The ARMON is a portable instrument based on method
201 C, consisting of alpha spectrometry of positive ions of ^{218}Po electrostatically collected on a detector
202 (Hopke, 1989). A detailed description of the ARMON is presented by Grossi et al. (2012).

203 Sampled air with a flow rate between $1\text{--}2\text{ L min}^{-1}$, is first filtered to remove ambient ^{222}Rn and ^{220}Rn
204 progeny and then pumped through a $\sim 20\text{ L}$ spherical detection volume uniformly covered internally with
205 silver. Within this volume the newly formed ^{222}Rn and ^{220}Rn progeny, i.e. positive ^{218}Po and ^{216}Po ions,
206 respectively, are electrostatically collected on a Passivated Implanted Planar Silicon (PIPS) detector
207 surface by an electrostatic field inside the spherical volume. An 8 kV potential is applied between the
208 PIPS detector base and the sphere walls. As for the ANSTO detector, the sensitivity of this instrument
209 type depends on the detector volume. The design of the monitor employed in this study allows a
210 minimum detectable activity concentration of about 0.2 Bq m^{-3} (Grossi et al., 2012). The measurement
211 efficiency of the electrodeposition method is reduced due to neutralization of the positive ^{218}Po in
212 recombination with OH^- ions in the sampled air (Hopke, 1989). Consequently, it is necessary to dry the
213 sampled air as much as possible before it enters the detection volume. To this end, a dew point of $< -40^\circ\text{C}$
214 was maintained at both intercomparison sites using a cryocooler.

215 Each ARMON is calibrated at the INTE-UPC ^{222}Rn chamber (Vargas et al., 2004) under different ^{222}Rn
216 and relative humidity conditions (Grossi et al., 2012). The radon chamber of the INTE-UPC is a 20 m^3
217 installation, which allows control of the exhalation rate ($0\text{--}256\text{ Bq min}^{-1}$) and the ventilation air flow rate
218 ($0\text{--}100\text{ L min}^{-1}$). The ^{222}Rn source is a dry powder material containing $2100\text{ kBq }^{226}\text{Ra}$ activity enclosed in
219 the source container (RN-1025 model manufactured by Pylon Electronics). The calibration factor F_{cal} of



220 the ARMON used in this study was of 0.39 counts per minute (cpm) per Bq m⁻³ with an uncertainty of
 221 10%. The correction factor for the humidity influence inside the sphere was of 6.5·10⁻⁵ per part per
 222 million H₂O (ppm) with an maximum uncertainty of 10%. The total uncertainty of the atmospheric radon
 223 activity concentration measured by the ARMON is of 20%. Every 1-2 years the progeny filter at the
 224 ARMON inlet should be changed.

225

Monitor	Method	α Spectrum	Flow Rate (L min ⁻¹)	Detection Limit (Bq m ⁻³)	Typical uncertainty	Remote Control	Need of dry air sample	Need of corrections depending on the height of the inlet	Portability Level	References
ANSTO	Dual- flow- loop two- filter	No	~83	0.03	8-12%	Yes	No	No	Low	Whittlestone and Zahorowski (1998); Brunke et al. (2002)
ARMON	Electrostatic deposition	Yes	1-2	~0.2	20%	Yes	Yes	No	Medium	Grossi et al. (2012)
HRM	One- filter	Yes	20	~0.05	15-20%	Yes	No	Yes	High	Levin et al. (2002)
LSCE	One- filter	Yes	160	~0.01	20%	Yes	No	Yes	High	Polian, 1986; Biraud, 2000

226 Table 1. Summary of principal characteristics of the ²²²Rn and ²²²Rn progeny monitors compared in the
 227 present study.

228 2.2 Sites

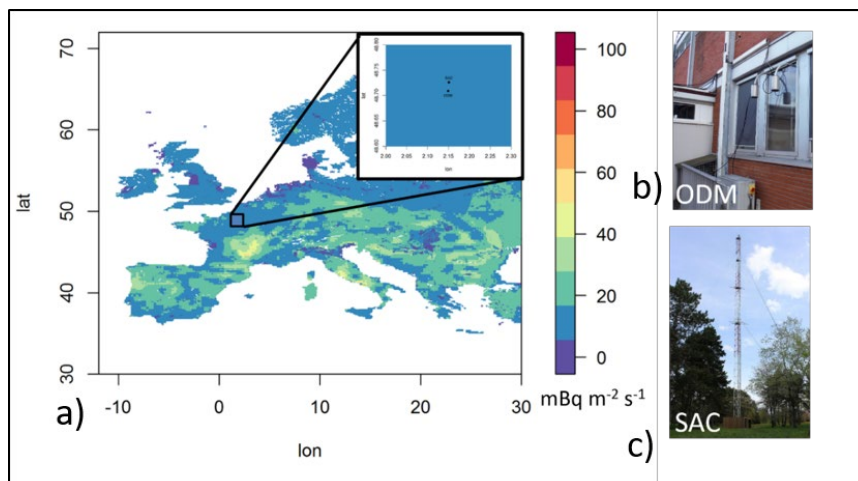
229 The intercomparison study was carried out at two stations located 30 km southwest of Paris in the fall and
 230 winter of 2016-2017 (Figure 1). Both stations, 3.5 km apart, belong to the LSCE and are located in a
 231 region with a radon flux of ca. 5-10 mBq m⁻² s⁻¹ in winter, according to output of the Karsten et al. (2015)
 232 model.

233 Phase I of the measurements started at Orme des Mérisiers (ODM, latitude 48.698, longitude 2.146, 167
 234 m above sea level) and ran between 25 November 2016 and 23 January 2017. Here, LSCE and ANSTO
 235 (for convenience named here as ANSTO_ODM) monitors are routinely running. During Phase I of the
 236 intercomparison exercise these two monitors were operated in parallel with a HRM and an ARMON. The
 237 sampling height for all radon detectors at ODM was 2 m a.g.l.

238 Phase II of the exercise was realized at Saclay (SAC, latitude 48.730, longitude 2.180, Figure 1) between
 239 25 January 2017 and 13 February 2017. At this location the sampling inlet height was at 100 m a.g.l. At
 240 SAC station an ANSTO monitor (from now on labelled as ANSTO_SAC) was already running. In
 241 addition, during Phase II this detector was running in parallel with the portable ARMON and HRM
 242 detectors. The LSCE monitor did not participate in Phase II of the experiment.



243 Meteorological parameters were also available at both stations during the intercomparison periods at
244 heights corresponding to the radon measurements (2 m and 100 m a.g.l.). In the case of the ODM site,
245 atmospheric aerosol concentrations were also measured for this period.



246

247 Figure 1. The INGOSv2.0 ^{222}Rn flux map (Karstens et al., 2015) is shown for a typical winter month
248 (December), with locations of the ODM and SAC sites shown in the inset (a). The radon sampling inlets
249 are shown both for ODM (b) and SAC (c).

250 2.3 Environmental parameters and atmospheric aerosol concentration

251 Meteorological data used within this study were variables because continuously measured at the SAC and
252 ODM stations at different heights. The measurements are carried out with a Vaisala Weather Transmitter
253 WXT520 (Campbell Scientific) for: (1) wind speed and direction (accuracies of $\pm 3\%$ and $\pm 3^\circ\text{C}$,
254 respectively); (2) Humidity and temperature (accuracies of $\pm 3\%$ and $\pm 0.3^\circ\text{C}$, respectively). In addition,
255 the atmospheric aerosol concentration is measured at ODM site using a Fine dust measurement device
256 Fidas® 200 S (Palas). The measurement range is between 0 and 20.000 particles cm^{-3} . All the accuracies
257 refer to the manufacturer's specifications.

258

259 2.4 Data Analysis

260 2.4.1 Correlation factors between monitors

261 In order to study the correlation between responses of the different detectors, linear regression models
262 were calculated using hourly atmospheric radon activity concentrations from each monitor. The linear
263 regression fits were calculated following Krystek and Anton (2007), relative to the two portable detectors,
264 ARMON and HRM, because they both were measuring at SAC and at ODM.

265



266 **2.4.2 Analysis of the influence of the environmental and meteorological parameters on detector**
267 **response**

268 The present study intended to build upon the findings of Xia et al. (2010) and Schmithüsen et al., (2017)
269 regarding the possible influence of meteorological conditions on the response of radon and radon progeny
270 monitors.

271 With this in mind, the ratio between hourly atmospheric ^{222}Rn activity concentrations measured and/or
272 obtained by the HRM, LSCE and ANSTO monitors, and that measured by the ARMON were calculated,
273 and their variability analyzed in relation to hourly atmospheric temperature, relative humidity and
274 atmospheric aerosol concentration measured at ODM and at SAC, respectively. For this part of the study,
275 the ARMON was used as reference being the only portable direct radon monitor running at both sites.

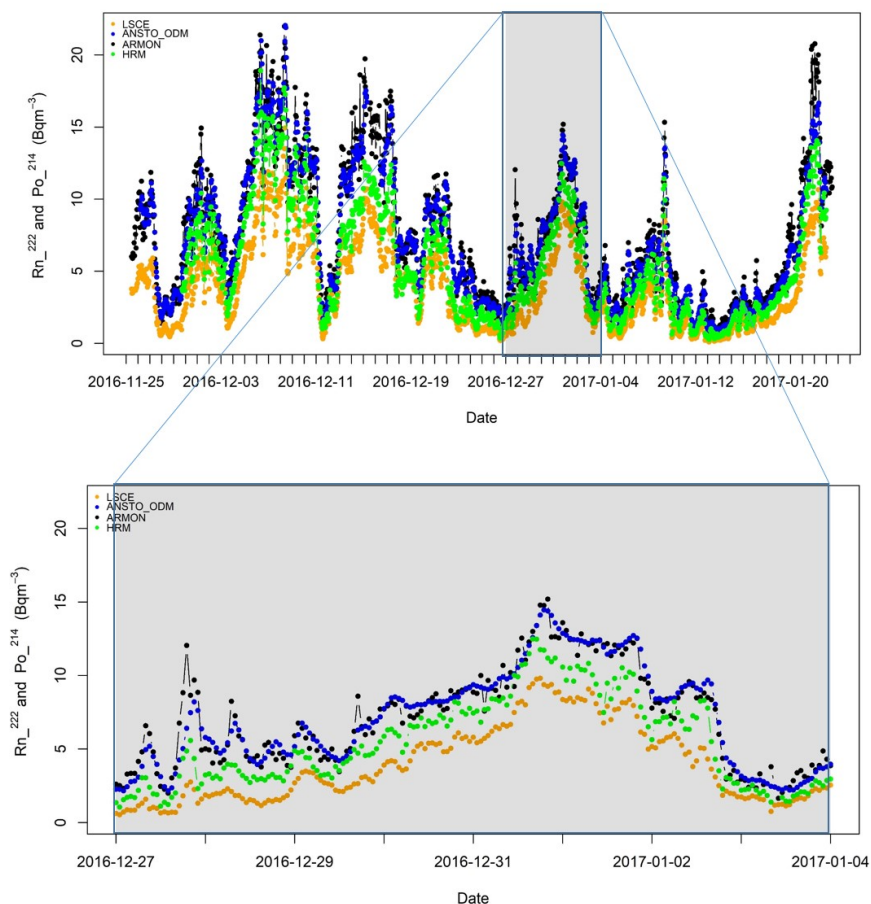
276 **3 Results**

277 Hourly time series of atmospheric ^{222}Rn , in the case of ARMON and ANSTO monitors, and ^{222}Rn
278 progeny (^{214}Po activity concentration) for the HRM and LSCE monitors, measured at ODM and SAC
279 during Phase I and Phase II of the intercomparison experiment are presented in Figures 2 and 3,
280 respectively. In each of the previous Figures, a zoom plot has been also reported as example to look at the
281 response of each monitor to the sub-diurnal atmospheric radon variability. As shown, all monitors
282 running at both sites follow this variability, with ^{222}Rn and ^{222}Rn progeny data measured or estimated by
283 the three different measurement techniques showing the same general patterns. Table 2 summaries the
284 means, minima and maxima hourly atmospheric radon or radon progeny activity concentrations measured
285 by each monitor for both campaigns.

286 **3.1 Phase I: ODM site**

287 During Phase I the LSCE, HRM, ARMON and ANSTO_ODM monitors were operating in parallel,
288 sampling air from the same height (2 m a.g.l.). The mean temperature over Phase I of the campaign was
289 2.9 °C with an interquartile range of 0.10 °C to 5.8 °C. The mean relative humidity was 80% with an
290 interquartile range of 73% to 89%. An average accumulated rain per day of 13 mm was recorded. The
291 main wind patterns during Phase I were from northeast and southwest, with speeds typically between 1
292 and 7 m s⁻¹. The mean atmospheric aerosol concentration observed at ODM during Phase I was 505
293 particles cm⁻³ with an interquartile range of 233 cm⁻³ to 660 cm⁻³.

294 The means of the atmospheric ^{222}Rn activity concentration measured by the ARMON and the
295 ANSTO_ODM are in the same order (Table 2). The means of the atmospheric radon daughter activity
296 concentrations measured by LSCE monitor is ca. 50% lower and by the HRM is ca. 30% lower than the
297 atmospheric ^{222}Rn activity concentration.



298

299

300 Figure 2. Main panel: Hourly time series of the atmospheric ^{222}Rn and, in the case of LSCE and HRM
301 data ^{214}Po activity concentration measured at Orme de Merisiers (ODM) station during Phase I (between
302 25 November 2016 and 23 January 2017) by: ARMON (black circles), ANSTO_ODM (blue circles),
303 HRM (green circles) and LSCE (orange circles) monitors. Zoomed panel: Hourly time series of the
304 atmospheric ^{222}Rn and ^{214}Po measured between 27th December 2016 and 04th January 2017.

305 Table 2 shows the slopes (b) and intercepts (a) of the linear regression fits calculated between the hourly
306 atmospheric ^{222}Rn and ^{214}Po activity concentrations measured by the ARMON and/or the HRM and the
307 other ^{222}Rn and ^{222}Rn progeny monitors deployed in Phase I. The calculated slopes were in the range of
308 0.62 to 1.17 and the R^2 values varied between 0.90 and 0.96. The slope closest to unity was calculated
309 between the ARMON and ANSTO_ODM monitors, and was 0.96 ± 0.01 , while the lowest slope was
310 observed between the ARMON and LSCE monitors, and was 0.62 ± 0.01 . The highest correlation
311 ($R^2=0.96$) was found between the HRM and LSCE monitors. The plots of the linear regression fits of the
312 Phase I are shown in the Figures S1, S2 and S3 left panel of the supporting material. Notably, the offset (a



313 value) of the regression between the ANSTO and ARMON detectors at ODM is considerably greater than
 314 that at SAC. The regression slopes are also slightly different, though not significantly so. These
 315 differences are likely related to the limited calibration and background information available for the
 316 ANSTO_ODM detector for this intercomparison project. In particular, a substantial component of the
 317 instrumental background signal is site specific. This is likely responsible for much of the change in offset
 318 value.

Monitors Phase I	Mean (Bq m ⁻³)	Min/Max (Bq m ⁻³)	x					
			b (ARMON)	a (ARMON)	R ² (ARMON)	b (HRM)	a (HRM)	R ² (HRM)
ANSTO_ODM	7.02	0.73/22.04	0.96±0.01	-0.23±0.03	0.94	1.17±0.01	0.63±0.03	0.93
HRM	5.45	0.26/18.91	0.82±0.01	-0.71±0.03	0.93	-	-	-
ARMON	7.55	0.50/21.98	-	-	-	-	-	-
LSCE	3.84	0.10/14.93	0.62±0.01	-0.85±0.03	0.90	0.76±0.004	-0.29±0.03	0.96
Monitors Phase II	Mean (Bq m ⁻³)	Min/Max (Bq m ⁻³)	Slope (ARMON)	Intercept (ARMON)	R ² (ARMON)	Slope (HRM)	Intercept (HRM)	R ² (HRM)
ANSTO_SAC	3.50	0.43/10.71	0.97±0.01	0.01±0.06	0.95	1.03±0.01	0.15±0.06	0.90
HRM	3.26	0.26/11.15	0.94±0.01	-0.13±0.06	0.91	-	-	-
ARMON	3.60	0.17/11.51	-	-	-	-	-	-

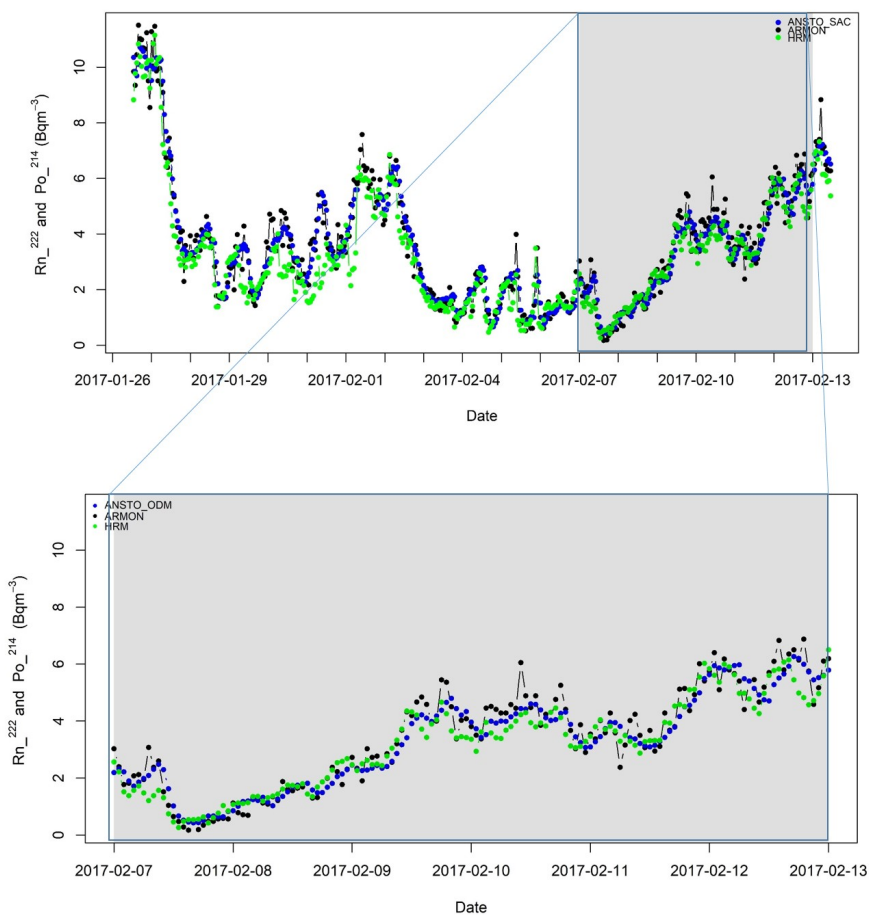
319

320 Table 2. The means, maxima, and minima of the atmospheric ²²²Rn and ²¹⁴Po activity concentration
 321 observed by each monitor participating in the Phase I and II of the intercomparison campaigns. In
 322 addition are here reported the slopes (*b*) and intercepts (*a*) of the linear regression fits calculated between
 323 the hourly atmospheric ²²²Rn and ²¹⁴Po activity concentrations measured by the ARMON and/or the HRM
 324 and the other ²²²Rn and ²²²Rn progeny monitors deployed in both phases.

325 3.2 Phase II: SAC station

326 Phase II lasted 18 days. The mean temperature during this period was 5 °C with an interquartile range of 2
 327 °C to 8 °C. The mean relative humidity was 86% with an interquartile range of 80% to 94%. An average
 328 accumulated rain per day of 3 mm was recorded. The main wind patterns during this phase at 100 m a.g.l.
 329 were from the south and southwest with speeds typically between 3 and 10 m s⁻¹.

330 Figure 3 shows the hourly atmospheric ²²²Rn and ²¹⁴Po activity concentrations observed at SAC during
 331 Phase II by the ARMON, HRM and ANSTO_SAC instruments. Table 2 reports the means, minima, and
 332 maxima of the atmospheric data measured during Phase II by all participating monitors. In this case, the
 333 mean atmospheric ²²²Rn and ²¹⁴Po activity concentrations measured by all monitors agreed within the
 334 instruments errors. At 100 m a.g.l. the slopes of the hourly fits of the monitor's response in this case were
 335 all close to unity. The calculated offsets also decreased at 100 m a.g.l. relative to 2 m a.g.l. The plots of
 336 the linear regression fits of Phase II are shown in the Figures S3 right panel and S4 of the supporting
 337 material.



338

339 Figure 3. Main panel: Hourly time series of the atmospheric ^{222}Rn and ^{214}Po (HRM) activity concentration
340 measured at Saclay (SAC) station between 25 January 2017 and 13 February 2017 by: ARMON (black
341 circles), ANSTO_SAC (blue circles) and HRM (green circles) monitors. Zoomed panel: Hourly time
342 series of the atmospheric ^{222}Rn and ^{214}Po measured between 7 February 2017 and 13 February 2017.

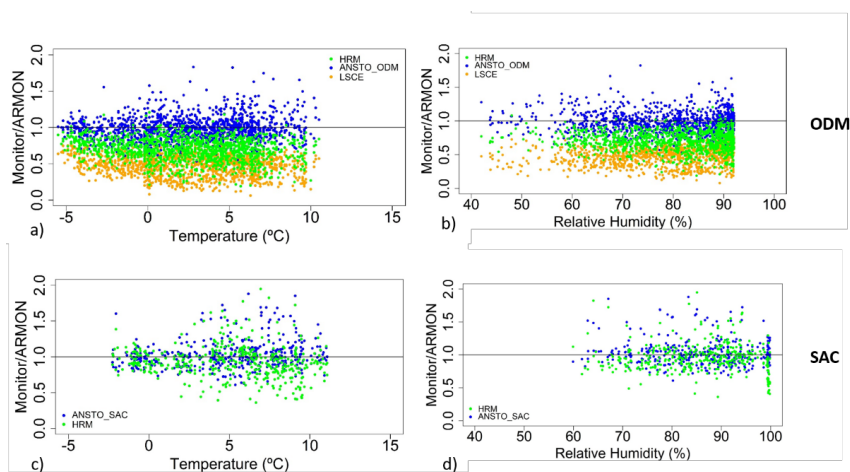
343 Figure 2 and 3 show a larger hourly variability of the HRM and ARMON signals compared with the
344 ANSTO ones. This difference in variability is attributable to the combination of a larger counting
345 uncertainty of the HRM and ARMON detectors, and that only an approximated response time correction
346 could be applied to the output of the ANSTO detectors (Griffiths et al. 2016). Further investigations
347 should be carried out to clarify these differences and to exactly quantify the detectors uncertainties for the
348 low ^{222}Rn concentrations typical for outdoor environmental monitoring at or above 100 m a.g.l. During
349 the period of Jan 30 – February 1, 2019, the HRM shows significantly lower values than the ANSTO and
350 ARMON. This period coincides with saturated air humidity conditions.

351



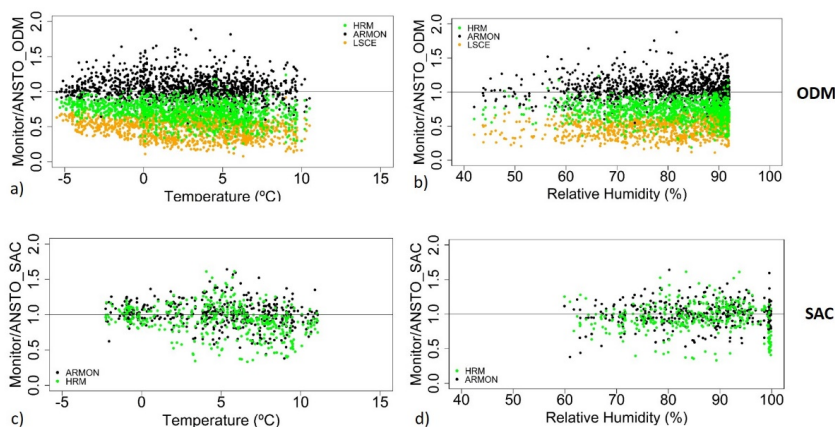
352 **3.3 Influence of the weather conditions on the ratio between direct ^{222}Rn and ^{214}Po measurements**

353 Figure 4 and 5 show the variability of the ratio between hourly atmospheric ^{222}Rn and/or ^{214}Po activity
354 concentration measured by each monitor relative to those measured by the ARMON at ODM (Figure 4,
355 upper panels) and at SAC (Figure 4, bottom panels) and by the ANSTO_ODM at ODM (Figure 5, upper
356 panels) and by the ANSTO_SAC at SAC (Figure 5, bottom panels) versus the hourly means of ambient
357 temperature (Figures 4 and 5, left panels) and relative humidity (Figures 4 and 5, right panels) measured
358 at the corresponding stations. Data does not show any evident patterns, which could indicate that there is
359 any impact on ^{222}Rn or ^{222}Rn progeny measurements due to change of ambient temperature and relative
360 humidity, at least not until saturated conditions are achieved. Looking at Figure 5, there appears to be less
361 scatter in the point clouds (particularly at SAC) when the ANSTO_SAC monitor is used as the reference,
362 likely attributable to the lower measurement uncertainty of the ANSTO monitors.



363

364 Figure 4. Hourly atmospheric ^{222}Rn or ^{214}Po activity concentration obtained by HRM, LSCE and ANSTO
365 monitors divided by the ^{222}Rn activity concentration measured by the ARMON detector as function of the
366 hourly measured atmospheric temperature and relative humidity at ODM (a and b) and at SAC (c and d),
367 respectively.



368

369 Figure 5. Hourly atmospheric ^{222}Rn or ^{214}Po activity concentration obtained by ARMON, HRM and
 370 LSCE monitors divided by the ^{222}Rn activity concentration measured by the ANSTO detectors as function
 371 of the hourly measured atmospheric temperature and relative humidity at ODM (a and b) and at SAC (c
 372 and d), respectively.

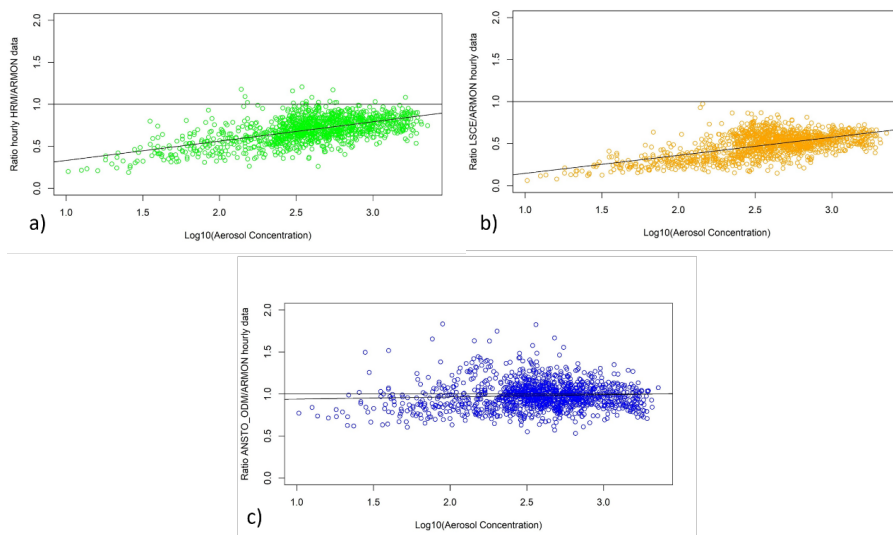
373

374 In Figure 6 the ratio of the hourly atmospheric ^{222}Rn or ^{222}Rn progeny activity concentration measured by
 375 the HRM (^{214}Po in Figure 6a), the LSCE (^{214}Po in Figure 6b) and the ANSTO_ODM (^{222}Rn in Figure 6c)
 376 monitor and the ^{222}Rn activity concentration measured with ARMON (^{222}Rn) are plotted against the
 377 logarithm of the hourly aerosol concentration data. Data indicate the existence of a linear relationship
 378 between these variables, i.e. of the form:

$$379 \frac{{}^{222}\text{Rn}(\text{Monitor}_i)}{{}^{222}\text{Rn}(\text{ARMON})} = a + b \cdot \text{Log}_{10}(\text{Aerosol Conc.}). \quad (1)$$

380 Here ${}^{222}\text{Rn}(\text{Monitor}_i)$ is the hourly atmospheric ^{222}Rn or ^{214}Po activity concentration measured by
 381 individual monitors HRM (^{214}Po), LSCE (^{214}Po) and ANSTO_ODM (^{222}Rn), ${}^{222}\text{Rn}(\text{ARMON})$ is the one
 382 measured by the ARMON monitor and *Aerosol Conc.* is the hourly atmospheric aerosol concentration
 383 measured at ODM during Phase I. The results of the linear regression fits for each compared monitor are
 384 reported in Table 3. The slope of the ratio between the ANSTO_ODM and ARMON monitors in relation
 385 to the variability of the logarithm of the hourly atmospheric aerosol concentration is close to zero and the
 386 intercept is close to one. The ratio between the hourly atmospheric aerosol-bound radon progeny data
 387 measured by the two one-filter radon progeny monitors and the one measured by the ARMON seems to
 388 decrease with decreasing aerosol concentration (Figures 6a and 6b). However, this effect becomes only
 389 evident when atmospheric aerosol concentration is lower than $300 \text{ particles cm}^{-3}$.

390



391

392 Figure 6. Ratio of the atmospheric ^{222}Rn or ^{214}Po activity concentration measured by the HRM (green
 393 dots), LSCE (orange dots) and ANSTO_ODM (blue dots) monitors and those measured by the reference
 394 ARMON monitor against the logarithm of the atmospheric aerosol concentration measured at ODM
 395 station.

Monitor	<i>a</i>	<i>b</i>	R^2
HRM	0.10 ± 0.02	0.23 ± 0.01	0.34
LSCE	-0.07 ± 0.02	0.21 ± 0.01	0.34
ANSTO_ODM	0.91 ± 0.03	0.03 ± 0.01	$0.04 \cdot 10^{-1}$

396

Table 3. Intercepts and slopes of the linear regression fits of the Equation 1

397 Conclusions

398 In order to confirm and build upon the results obtained by Xia et al. (2010), Grossi et al. (2016) and
 399 Schmithüsen et al. (2017) a three months intercomparison campaign was carried out in the south of Paris,
 400 France, in the fall-winter period of 2016-2017. For the first time, three fundamentally distinct radon and
 401 radon progeny measurement approaches deployed at GHG observation sites across Europe were
 402 compared side-by-side at two measurement heights: 2 and 100 m a.g.l., under a range of environmental
 403 conditions with the aim to compare their responses under various atmospheric and/or meteorological
 404 conditions.

405 The results of this study show that ^{222}Rn and ^{222}Rn progeny measurements follow the same general
 406 patterns of diurnal variability, both close to and further up from the surface. The slopes and intercepts of
 407 the linear regression fits between the direct radon and the radon-progeny measurements are not
 408 significantly different from one at 100m height above ground (SAC), but they differ at the 2m level
 409 (ODM). This behavior is attributable to the disequilibrium known to exist between ^{222}Rn freshly emitted
 410 from the ground and its short-lived progeny in the lowest 10s of meters of the atmosphere, the magnitude



411 of which is known to decrease with distance from the surface, as shown in earlier work, and to be close to
412 one at a height of 100m and above (e.g. Jacobi and André, 1963; Schmithüsen et al., 2017).

413 For the 2 m level, we found a very good correlation of radon progeny activity concentrations between
414 LSCE and HRM measurements (see Figure S1 in the Supplement). The slope, however, is only equal to
415 0.76 ± 0.04 . This number is slightly larger but within uncertainties well comparable to the number reported
416 by Schmithüsen et al. (2017) of 0.68 ± 0.03 (see their Table 2) based on a comparison campaign conducted
417 at ODM in March and April 2014.

418 Observations of the total atmospheric aerosol concentration available at ODM station during the first two
419 months of the experiment were used to investigate the influence of changing atmospheric aerosol
420 concentrations on the response of the radon/radon progeny measurements. Under very low atmospheric
421 aerosol burden (< 300 particles cm^{-3}), the ^{222}Rn progeny monitors seem to underestimate the atmospheric
422 ^{214}Po activity concentrations by up to 50%. This effect may be attributable to loss of un-attached ^{218}Po
423 and ^{214}Po . Particle number concentrations below 300 particles cm^{-3} at continental stations are, however,
424 very rare and even during winter at Alpine stations like Schneefernerhaus such low particle
425 concentrations are only occasionally observed (Birmili et al., 2009).

426 Acknowledgments

427 The research leading to these results has received funding from the Ministerio Español de Economía y
428 Competitividad, Retos 2013 (2014–2016) with the MIP (Methane interchange between soil and air over the
429 Iberian Peninsula) project (reference: CGL2013-46186-R). This study was carried out under the umbrella
430 of the Atmospheric Thematic Center (ATC) of ICOS.

431 Claudia Grossi particularly thanks the Ministerio Español de Educación, Cultura y Deporte, for partially
432 supporting her work with the research mobility grant “José Castillejos” (ref. CAs15/00042).

433 The authors warmly thank (i) the INTE team, in the persons of Vicente Blasco and Juan Antonio Romero,
434 for their work in the building of the ARMON used in this study; (ii) the R project (www.r-project.org)
435 free software environment used here for statistical computing and graphics.

436 This paper is dedicated to: Bruno Grossi, Dr. Manuel Javier Navarro Angulo, Dr. Alfredo Adán and the
437 whole team of the Instituto Clínic de Oftalmología (ICOF) of the Hospital Clínic of Barcelona.

438 References

439 Baskaran, M.: Po-210 and Pb-210 as atmospheric tracers and global atmospheric Pb-210 fallout: a
440 Review. *J. of Environ. Radioact.* 102 (5), 500-513, doi: 10.1016/j.jenvrad.2010.10.007, 2010.

441 Baskaran, M.: Radon: A Tracer for Geological, Geophysical and Geochemical Studies” Springer
442 Geochemistry book series (SPRIGEO), 2016.

443 Biraud, S.: Vers la régionalisation des puits et sources des composés à effet de serre: analyse de la
444 variabilité synoptique à l’observatoire de Mace Head, Irlande, PhD Thesis, University of Paris VII,
445 France, 2000.



- 446 Birmili, W., L. Ries, R. Sohmer, A. Anastou, A. Sonntag, K. König, I. Levin, 2009b. Fine and ultrafine
447 aerosol particles at the GAW station Schneefernerhaus/Zugspitze. – *Gefährst. Reinh. Luft* 69(1/2), 31–35.
- 448 Chambers, S. D., A. G. Williams, W. Zahorowski, A. Griffiths, and J. Crawford: Separating remote fetch
449 and local mixing influences on vertical radon measurements in the lower atmosphere. *Tellus B*, 63(5),
450 843-859, doi: 10.1111/j.1600-0889.2011.00565.x, 2011.
- 451 Chambers, S. D., W. Zahorowski, A. G. Williams, J. Crawford, and A. D. Griffiths: Identifying
452 tropospheric baseline air masses at Mauna Loa Observatory between 2004 and 2010 using Radon-222 and
453 back trajectories, *J. Geophys. Res.: Atmos.*, 118(2), 992-1004, doi: 10.1029/2012JD018212, 2013.
- 454 Chambers, S. D., S. B. Hong, A. G. Williams, J. Crawford, A. D. Griffiths, and S. J. Park: Characterising
455 terrestrial influences on Antarctic air masses using Radon-222 measurements at King George Island,
456 *Atmos. Chem. Phys.*, 14, 9903-9916, doi:10.5194/acp-14-9903-2014, 2014.
- 457 Chambers, S. D., A. G. Williams, F. Conen, A. D. Griffiths, S. Reimann, M. Steinbacher, P. B. Krummel,
458 L. P. Steele, M. V. van der Schoot, I. E. Galbally, S. B. Molloy, and J. E. Barnes: Towards a universal
459 “baseline” characterisation of air masses for high- and low-altitude observing stations using Radon-222,
460 *Aerosol Air Qual. Res.*, 16, 885-899, doi: 10.4209/aaqr.2015.06.0391, 2015.
- 461 Chambers, S.D. D. Galeriu, A.G. Williams, A. Melintescu, A.D. Griffiths, J. Crawford, L. Dyer, M.
462 Duma, B. Zorila: Atmospheric stability effects on potential radiological releases at a nuclear research
463 facility in Romania: Characterising the atmospheric mixing state. *J. of Environ. Radioact.*, 154, 68-82,
464 doi: 10.1016/j.jenvrad.2016.01.010, 2016.
- 465 Chambers SD, Preunkert S, Weller R, Hong S-B, Humphries RS, Tositti L, Angot H, Legrand M,
466 Williams AG, Griffiths AD, Crawford J, Simmons J, Choi TJ, Krummel PB, Molloy S, Loh Z, Galbally I,
467 Wilson S, Magand O, Sprovieri F, Pirrone N and Dommergue A.: Characterizing Atmospheric Transport
468 Pathways to Antarctica and the Remote Southern Ocean Using Radon-222, *Front. Earth Sci.*, 6:190,
469 <https://doi.org/10.3389/feart.2018.00190>, 2018.
- 470 Chambers SD, Guérette E-A, Monk K, Griffiths AD, Zhang Y, Duc H, Cope M, Emmerson KM, Chang
471 LT, Silver JD, Utembe S, Crawford J, Williams AG and Keywood M.: Skill-testing chemical transport
472 models across contrasting atmospheric mixing states using Radon-222, *Atmosphere* 10 (1), 25;
473 <https://doi.org/10.3390/atmos10010025>, 2019a
- 474 Chambers SD, Podstawczyńska A, Pawlak W, Fortuniak K, Williams AG and Griffiths AD.:
475 Characterising the state of the urban surface layer using Radon-222, *J. Geophys. Res. Atmos.*, 124(2),
476 770-788, <https://doi.org/10.1029/2018JD029507>, 2019b.
- 477 Frank, G., Salvamoser, J., and Steinkopf, T.: Messung radioaktiver Spurenstoffe in der Atmosphäre im
478 Rahmen des Global Atmosphere Watch Programmes der WMO, Umweltforschungsstation
479 Schneefernerhaus, Wissenschaftliche Resultate 2011/2012,
480 http://www.schneefernerhaus.de/fileadmin/web_data/bilder/pdf/UFS-Broschuere_2012.pdf, last access:
481 18 August, 2016.



- 482 Galmarini, S.: One year of ^{222}Rn concentration in the atmospheric surface layer, *Atmos. Chem. Phys.*, 6,
483 2865-2887, doi: 10.5194/acp-6-2865-2006, 2006.
- 484 Griffiths, A. D., Chambers, S. D., Williams, A. G., and Werczynski, S.: Increasing the accuracy and
485 temporal resolution of two filters radon-222 measurements by correcting for the instrument response,
486 *Atmos. Meas. Tech.*, 9, 2689–2707, doi:10.5194/amt-9-2689-2016, 2016.
- 487 Grossi, C., Arnold, D., Adame, A. J., Lopez-Coto, I., Bolivar, J. P., de la Morena, B. A., and Vargas, A.:
488 Atmospheric ^{222}Rn concentration and source term at El Arenosillo 100m meteorological tower in
489 southwest, Spain. *Radiat. Meas.*, 47, 149–162, doi:10.1016/j.radmeas.2011.11.006, 2012.
- 490 Grossi, C., Àgueda, A., Vogel, F. R., Vargas, A., Zimnoch, M., Wach, P., Martín, J. E., López-Coto, I.,
491 Bolívar, J. P., Morguá, J.-A., and Rodó, X.: Analysis of ground-based ^{222}Rn measurements over Spain:
492 filling the gap in southwestern Europe, *J. Geophys. Res.-Atmos.*, 121, 11021–11037,
493 <https://doi.org/10.1002/2016JD025196>, 2016.
- 494 Grossi, C., Vogel, F. R., Curcoll, R., Àgueda, A., Vargas, A., Rodó, X., and Morguá, J.-A.: Study of the
495 daily and seasonal atmospheric CH_4 mixing ratio variability in a rural Spanish region using ^{222}Rn tracer,
496 *Atmos. Chem. Phys.*, 18, 5847-5860, <https://doi.org/10.5194/acp-18-5847-2018>, 2018.
- 497 Gutiérrez-Álvarez, I. Guerrero, J. L. Martín, J. E. Adame, J. A. Vargas, A. Bolívar, J. P.: Radon behavior
498 investigation based on cluster analysis and atmospheric modelling, *Atm. Environ.* 201, 50-61, doi:
499 10.1016/j.atmosenv.2018.12.010, 2019.
- 500 Hernández-Ceballos, M. A., A. Vargas, D. Arnold, and J. P. Bolívar: The role of mesoscale meteorology
501 in modulating the ^{222}Rn concentrations in Huelva (Spain) - impact of phosphogypsum piles, *J. Environ.*
502 *Radioact.*, 145, 1-9, doi: 10.1016/j.jenvrad.2015.03.023, 2015.
- 503 Hirao, S., H. Yamazawa, and J. Moriizumi: Inverse modelling of Asian ^{222}Rn flux using surface air
504 ^{222}Rn concentration, *J. Environ. Radioact.*, 101(11), 974-984, doi: 10.1016/j.jenvrad.2010.07.004, 2010.
- 505 Hopke, P. K.: The initial behavior of ^{218}Po in indoor air. *Environment International*, 15, 299-308, 1989.
- 506 Jacobi, W. and André, K.: The vertical distribution of Radon 222, Radon 220 and their decay
507 products in the atmosphere, *J. Geophys. Res.*, 68, 3799–3814, 1963.
- 508 IAEA (International Atomic Energy Agency): Sources and Measurements of Radon and Radon Progeny
509 Applied to Climate and Air Quality Studies. Proceedings of a technical meeting held in Vienna, organized
510 by the International Atomic Energy Agency and co-sponsored by the World Meteorological Organization,
511 IAEA, Austria, Vienna, 2012.
- 512 Krystek, M. and Anton, M. 2007. A weighted total least-squares algorithm for fitting a straight line.
513 *Meas. Sci. Technol.* 18, 3438–3442, doi:10.1088/0957-0233/18/11/025
- 514 Levin, I., H. Glatzel-Mattheier, T. Marik, M. Cuntz, M. Schmidt, and D. E. J. Worthy: Verification of
515 German methane emission inventories and their recent changes based on atmospheric observations, *J.*
516 *Geophys. Res.*, 104(D3), 3447-3456, doi: 10.1029/1998JD100064, 1999.



- 517 Levin, I., Hammer, S., Eichelmann, E. and Vogel, F.R.: Verification of greenhouse gas emission
518 reductions: the prospect of atmospheric monitoring in polluted areas. *Philosophical Transactions of the*
519 *Royal Society of London A: Mathematical, Physical and Engineering Sciences*, 369(1943),1906-1924,
520 2011
- 521 Levin, I., Born, M., Cuntz, M., Langendörfer, U., Mantsch, S., Naegler, T., Schmidt, M., Varlagin, A.,
522 Verclas, S., and Wagenbach, D.: Observations of atmospheric variability and soil exhalation rate of
523 Radon-222 at a Russian forest site: Technical approach and deployment for boundary layer studies, *Tellus*
524 *B*, 54, 462–475, 2002.
- 525 Levin, I., Schmithüsen, D., and Vermeulen, A.: Assessment of 222radon progeny loss in long tubing
526 based on static filter measurements in the laboratory and in the field, *Atmos. Meas. Tech.*, 10, 1313–1321,
527 doi:10.5194/amt-10-1313-2017, 2017.
- 528 Locatelli, R., P. Bousquet, F. Hourdin, M. Saunois, A. Cozic, F. Couvreux, J. Y. Grandpeix, M. P.
529 Lefebvre, C. Rio, P. Bergamaschi, S. D. Chambers, U. Karstens, V. Kazan, S. van der Laan, H. A. J.
530 Meijer, J. Moncrieff, M. Ramonet, H. A. Scheeren, C. Schlosser, M. Schmidt, A. Vermeulen, and A. G.
531 Williams: Atmospheric transport and chemistry of trace gases in LMDz5B: evaluation and implications
532 for inverse modelling, *Geosci. Model Dev.*, 8, 129–150, doi: 10.5194/gmd-8-129-2015, 2015.
- 533 López-Coto, I., Mas, J.L., Bolivar, J.P.: A 40-year retrospective European radon flux inventory including
534 climatological variability, *Atmos. Environ.*, 73, 22–33, doi: 10.1016/j.atmosenv.2013.02.043, 2013.
- 535 Nazaroff, W.W., and Nero, A.V. (Eds.): *Radon and its decay products in indoor air*, John Wiley & Sons,
536 New York, USA, doi: 10.1063/1.2810982, 1988.
- 537 Karstens, U., Schwingshackl, C., Schmithüsen, D., and Levin, I.: A process-based 222radon flux map for
538 Europe and its comparison to long-term observations, *Atmos. Chem. Phys.*, 15, 12845-12865,
539 <https://doi.org/10.5194/acp-15-12845-2015>, 2015.
- 540 Paatero, J., Hatakka, J., and Viisanen, Y.: Concurrent measurements of airborne radon-222, lead-210 and
541 beryllium-7 at the Pallas-Sodankylä GAW station, Northern Finland, Reports 1998:1, Finnish
542 Meteorological Institute, Helsinki, 1998.
- 543 Schery, S. D. and Huang, S.: An estimate of the global distribution of radon emissions from the ocean,
544 *Geophys. Res. Lett.*, 31, L19104, doi:10.1029/2004GL021051, 2004.
- 545 Schmithüsen, D., Chambers, S., Fischer, B., Gilge, S., Hatakka, J., Kazan, V., Neubert, R., Paatero, J.,
546 Ramonet, M., Schlosser, C., Schmid, S., Vermeulen, A., and Levin, I.: A European wide 222radon and
547 222radon progeny comparison study, *Atmos. Meas. Tech.*, 10, 1299–1312, [https://doi.org/10.5194/amt-](https://doi.org/10.5194/amt-10-1299-2017)
548 10-1299-2017, 2017.
- 549 Stockburger, H. und Sittkus, A.: Unmittelbare Messung der natürlichen und künstlichen Radioaktivität
550 der atmosphärischen Luft, *Zeitschrift für Naturforschung*, 21, 1128–1132, 1966.



- 551 Szegvary, T., Conen, F. Ciaia, P.: European 222Rn inventory for applied atmospheric studies, *Atmos.*
552 *Environ.*, 43(8), 1536–1539, doi: 10.1016/j.atmosenv.2008.11.025, 2009.
- 553 Vargas, A., D. Arnold, J. A. Adame, C. Grossi, M. A. Hernández-Ceballos, and J. P. Bolívar: Analysis of
554 the vertical radon structure at the Spanish “El Arenosillo” tower station, *J. Environ. Radioact.*, 139, 1-17,
555 doi: 10.1016/j.jenvrad.2014.09.018, 2015.
- 556 Vogel, F.R., M. Ishizawa, E. Chan, D. Chan, S. Hammer, I. Levin, and D. E. J. Worthy: Regional non-
557 CO₂ greenhouse gas fluxes inferred from atmospheric measurements in Ontario, Canada, *J. Integr.*
558 *Environ. Sci.*, 9 (S1), 1-15, doi: 10.1080/1943815X.2012.691884, 2012.
- 559 Vogel, F. R., B. Tiruchittampalam, J. Theloke, R. Kretschmer, C. Gerbig, S. Hammer, and I. Levin: Can
560 we evaluate a fine-grained emission model using high-resolution atmospheric transport modelling and
561 regional fossil fuel CO₂ observations?, *Tellus B*, 65, 18681, doi: 967
562 <http://dx.doi.org/10.3402/tellusb.v65i0.18681>, 2012.
- 563 Wada, A., H. Matsueda, S. Murayama, S. Taguchi, S. Hirao, H. Yamazawa, J. Moriizumi, K. Tsuboi, Y.
564 Niwa, and Y. Sawa: Quantification of emission estimates of CO₂, CH₄ and CO for East Asia derived
565 from atmospheric radon-222 measurements over the western North Pacific, *Tellus B*, 65, 18037, doi:
566 <http://dx.doi.org/10.3402/tellusb.v65i0.18037>, 2013.
- 567 Weller, R., Levin, I., Schmithüsen, D., Nachbar, M., Asseng, J., and Wagenbach, D. : On the variability
568 of atmospheric 222Rn activity concentrations measured at Neumayer, coastal Antarctica. *Atmos. Chem.*
569 *Phys.*, 14: 3843–3853, 2014.
- 570 Williams, A. G., W. Zahorowski, S. Chambers, A. Griffiths, J. M. Hacker, A. Element, and S.
571 Werczynski, S., The vertical distribution of radon in clear and cloudy daytime terrestrial boundary layers,
572 *J. Atmos. Sci.*, 68 (1), 155-174, doi: 10.1175/2010JAS3576.1, 2011.
- 573 Williams, A. G., S. Chambers, and A. Griffiths: Bulk mixing and decoupling of the nocturnal stable
574 boundary layer characterized using a ubiquitous natural tracer, *Boundary Layer Meteorol.*, 149(3), 381-
575 402, doi: 10.1007/s10546-013-9849-3, 2013.
- 576 Williams, AG and SD Chambers: A history of radon measurements at Cape Grim, *Baseline Atmospheric*
577 *Program (Australia) History and Recollections (40th Anniversary Special Edition)*, 131-146, 2016.
- 578 Whittlestone, S., and W. Zahorowski: Baseline radon detectors for shipboard use: Development and
579 deployment in the First Aerosol Characterization Experiment (ACE 1), *J. Geophys. Res.*, 103(D13),
580 16743–16751, doi: 10.1029/98JD00687, 1998.
- 581 Xia, Y., H. Sartorius, C. Schlosser, U. Stöhlker, F. Conen, and W. Zahorowski: Comparison of one- and
582 two-filter detectors for atmospheric 222Rn measurements under various meteorological conditions,
583 *Atmos. Meas. Tech.*, 3, 723-731, doi: 10.5194/amt-3-723-2010, 2010.



584 Zahorowski, W., S. D. Chambers, and A. Henderson-Sellers: Ground based radon-222 observations and
585 their application to atmospheric studies, *J. Environ. Radioact.*, 76(1-2), 3-33, doi:
586 10.1016/j.jenvrad.2004.03.033, 2004.

587 Zimnoch, M., P. Wach, L. Chmura, Z. Gorczyca, K. Rozanski, J. Godłowska, J. Mazur, K. Kozak, and A.
588 Jericevic: Factors controlling temporal variability of near-ground atmospheric ²²²Rn concentration over
589 central Europe. *Atmos. Chem. Phys.* 14, 9567–9581, doi: 10.5194/acp-14-9567-2014, 2014.

590

591

592